

On the Fracture of Pharmaceutical Needle-Shaped Crystals during Pressure Filtration: Case Studies and Mechanistic Understanding

Claire S. MacLeod* and Frans L. Muller

Pharmaceutical Development, AstraZeneca, Hulley Road, Macclesfield SK11 2NA, U.K.

ABSTRACT: Pharmaceutical compounds often crystallise as particles with high aspect ratio, typically as needle-shaped particles. These particles must be isolated from the crystallisation liquors before further secondary processing to form the drug product. A common isolation method in the fine chemical and pharmaceutical industries is pressure filtration. Previous experience has shown that, on scale-up from lab to pilot plant, the particle size distribution can change quite significantly. This has typically been associated with agitation of the filter cake. To test this assumption a number of industrial case studies were conducted. The particle size distribution of various needle-shaped particles of different pharmaceutical and model compounds have been tracked through the filtration and drying process. The work here shows that, for the needle-shaped particles tested, particle breakage occurs during both pressure filtration and agitated drying. This is a previously unreported observation and is contrary to the previously held assumption that breakage is only observed during agitated drying. A mechanistic understanding of the breakage has been built up using particle dimensions, applied pressure, and bed density. The estimated stresses on the needle-shaped particles are of the same order of magnitude as typical tensile strengths of pharmaceutical materials, thus explaining why breakage is observed. A small-scale test has been developed to help identify potentially fragile compounds where breakage during pressure filtration is likely.

■ INTRODUCTION

The development of pharmaceutical products is generally split in two distinct activities: (i) the development of the drug substance, that is the clinically active molecule (API) and (ii) the development of the formulated drug product, via which the drug substance is delivered to the patient.

The drug substance is typically generated by batch crystallisation. The crystallisation mass is transferred to a pressure filter where pressure is applied to separate the liquors from the solid. The drying procedure varies from company to company. The procedure used at AstraZeneca is to dry the filter cake by hot nitrogen or under vacuum, only switching on the agitator once the filter cake is almost dry. Before discharge the batch is agitated continuously for 15 min to ensure uniformity.

Particles produced from pilot-plant campaigns often have significantly smaller particle size than material isolated in the lab. This has been found to be due to attrition during agitated drying of the compound.^{1,2} However, this work differs because the evolution of particle size throughout the whole isolation process, from crystallizer to dried API, is studied. There is minimal coverage in the literature of the effect of particle properties, equipment scale, and manner of operation on the final particle size, especially on industrially relevant case studies.

Whereas a significant amount of development time is spent on designing the crystallisation process, and its scale-up is well understood (unless nucleation occurs³), scale-up of isolation processes is not well understood. There is a significant risk that the material properties of the final drug substance can vary from manufacture to manufacture. The nature of the drug substance is of course extremely important to those doing the formulation development as changes can impact on secondary processing. For instance the particle size distribution is known to affect

properties such as flowability, bulk density, and tableting performance.⁴

In order to better understand scale-up of filtration and drying with respect to the final drug substance particle size, we set out to investigate the degree to which particles fracture during the isolation process. Several case studies are presented of compounds that were filtered and dried in pressure filters, both at pilot plant and at representatively scaled-down lab scale. Samples taken throughout the isolation process were analysed for particle size, and this change in particle size tracked through the isolation process.

A common difficulty with this type of study is discerning between deagglomeration and fracture as means by which the measured particle size is reduced. Both hypotheses have been considered, and from the data presented, it is more likely that fracture is the cause of most of the decrease in particle size, although deagglomeration cannot be completely ignored.

The key observation was that both pressure filtration and agitation of the cake appear to cause breakage for this set of particles. A mechanistic model of particles in a filter bed and the effect of the pressure applied on those particles led to a qualitative model for the fracture of particles during pressure filtration. A small-scale test was developed on the basis of the pressure titration commonly used in particle sizing. This is the first, tentative attempt to relate this pressure titration data to the physical properties of particles.

■ EXPERIMENTAL METHODS

Materials. The following materials were used in this work: acetylsalicylic acid (aspirin), acetimophen (paracetamol),

Received: October 7, 2011

Published: February 2, 2012

acetanilide and glutamic acid all from Sigma-Aldrich. Four development compounds from AstraZeneca, AZ1, AZ2, AZ3 and AZ4, for which the structure cannot be disclosed were also used. The solvents used in this work are deionised Macclesfield tap water, ethanol and methanol. The solvents for the development compounds also cannot be revealed and are referred to as alcohol and ketone.

Crystallisation Process. A range of crystallisation processes has been executed to obtain a range of crystal shapes and sizes, shown in Table 1. At the lab scale, the solute is added

Table 1. Crystallisation processes used

cmpd	solvent	cryst'n cond'ns
AZ1	alcohol/water	slow cool
AZ2	water	acid addition
AZ3	alcohol/ketone	acid addition and cool
AZ4	alcohol/water	moderate cool
aspirin	38% aq ethanol	10 °C/min cool
paracetamol	25% aq methanol	0.2 °C/min cool
acetanilide	water	1 °C/min cool
glutamic acid	water	0.1 °C/min cool ^a

^aNeedles from micronized seed, rods from unmicronized seed.

to a large (typically 3000 mL) jacketed vessel fitted with an overhead stirrer and retreat curve agitator, a condenser, and a thermocouple. Solvent is added and the slurry heated to a batch

temperature high enough for complete dissolution. Super saturation is then generated by cooling and, in some cases, by acid addition. Table 1 gives the specific conditions for the case studies presented. The prepared crystallisation masses were used for the filtration studies. The crystallisation processes on the pilot-plant scale were carried out in a 1200-L crystalliser fitted with retreat curve agitator.

Filtration and Drying. The following filtration procedure was used. To determine the starting particle size distribution (PSD) of the crystallised mass, a small slurry sample was removed from the bulk and filtered on a small Buchner filter by application of ~0.2 barg vacuum, washed with a suitable solvent, and dried in a vacuum oven. This sample is denoted 'before filtration'. On the pilot plant, a small slurry sample was withdrawn from the pumped loop sampling system, and the slurry was filtered in the lab in the same manner as for the lab-scale process.

The remainder of the slurry was then transferred to a pressure filter. In the lab this is an 8-cm diameter pressure filter (GL Filtration Filter Lab 80), and on the pilot plant this is a 0.7-m diameter pressure filter (Rosenmund). The Filter Lab 80 has been designed as a scaled down version of the Rosenmund filter dryers used in pilot-plant facilities. A diagram is shown in Figure 1 with detail of the agitator. The agitator is a ploughing type agitator and is representative of the agitators used in pilot-plant facilities.

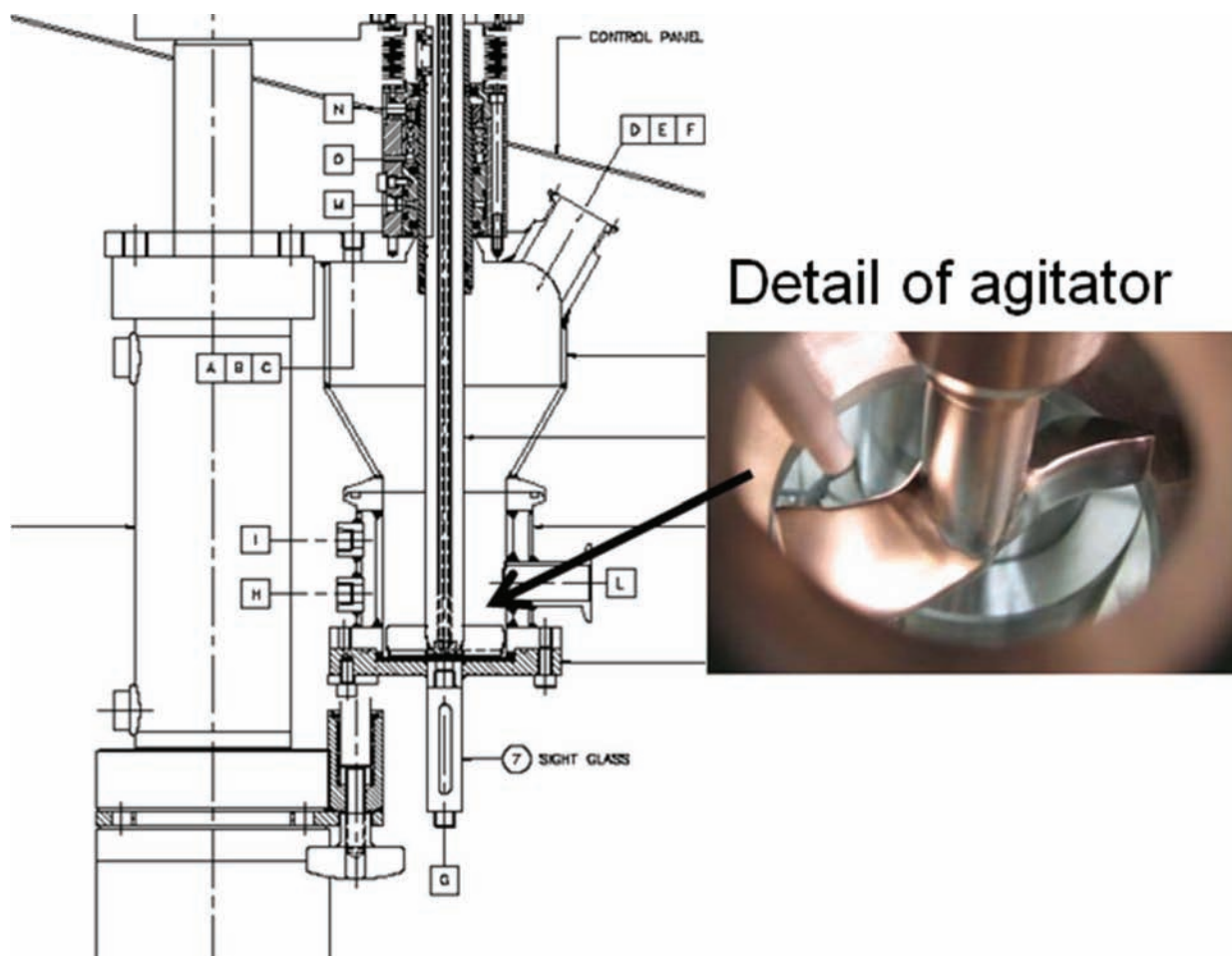


Figure 1. GL filtration filter lab 80.

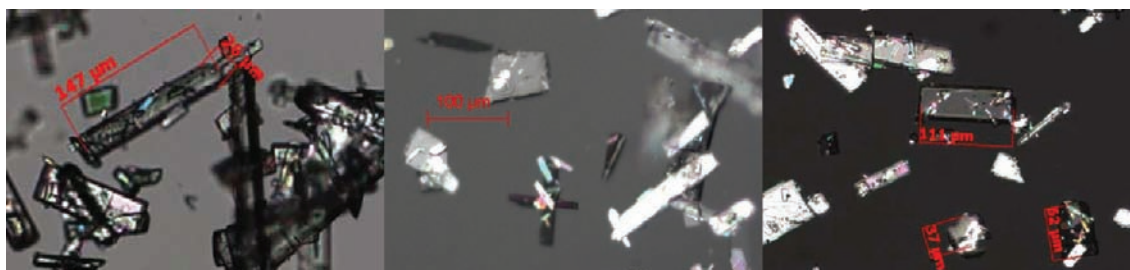


Figure 2. Microscope images (10 \times magnification) of AZ1 (left to right: before filtration, after filtration, and after agitation).

The slurry is filtered at 1.6 barg, and washed twice by charging a suitable solvent on top of the cake and letting it soak in without agitation (a ‘displacement’ wash). A small sample is then removed from the cake at this point and denoted ‘*after filtration*’. On the lab scale the sample is taken using a cork borer, sampling through the depth of the cake, then using a spatula to gently repair the hole in the cake. On the pilot plant the top of the cake is patted down briefly between the filtration and wash to prevent cracks forming. The sample is taken from a ball-valve type sampler below the level where the cake is patted down. In both cases the sampled particles have not been sheared by an agitator, so any changes in PSD are due to the filtration process.

The cake is then dried with flow-through nitrogen, and a further sample removed from the cake, denoted ‘*after drying*’. The nitrogen is heated to 40 °C at a flow rate of 1 m³/m²/s. This stage of drying typically takes between 8 and 12 h on the pilot plant and is left overnight in the lab. At this stage, in the lab the cake is typically completely dry, whereas on the pilot plant the cake could still be partially wet. Investigations on the effect of the extent of dryness on the likelihood of breakage being observed during agitation have not been conducted. It was found in the investigation by Lekhal^{2,5} that most of the attrition seen during agitated drying occurred at low moisture contents due to the absence of the solvent, which forms a lubricating barrier. Therefore, by completely drying the lab samples, it will be more likely that attrition is seen in the lab samples.

After this period of static drying the cake is agitated to improve the mass transfer. The samples from the pilot plant were agitated at 20 rpm, tip speed 0.7 m/s for a minimum of 15 min, and samples were taken after completion of the drying, denoted ‘*after agitation*’. The lab samples were agitated at 100 rpm (tip speed 0.4 m/s) and samples removed after 30 min and 2 h. The sample after 2 h is the ‘*after agitation*’ figure reported.

For all samples the PSDs were measured, and optical microscopy pictures were taken.

Particle Size Distribution. The PSDs of the samples were measured using laser diffraction (Sympatec’s HELOS detector) using dry dispersion (Rodos) with an Aspiris dispenser. Sample size was 200 mg. Samples were analysed in duplicate. This system gives a volume-weighted PSD curve. To get a consistent and observer-independent measure, the sample ‘before filtration’ was used to identify the particle sizes x_{25} and x_{75} that correspond to the initial 25% and 75% of the cumulative distribution, respectively. Due to the discrete nature of the PSD the actual values of the volume fractions associated with x_{25} and x_{75} are only approximately 25% or 75%. For instance for AZ1 it is 23%. For all PSDs, the fraction of small (f_s) and large (f_l) particles can then be found as the volume fraction of particles with $x < x_{25}$ and $x > x_{75}$ respectively.

Variable Pressure Attrition Test (VPAT). In dry dispersion particle sizing, a pressure titration is typically carried out to determine the dispersion pressure at which agglomerates are being broken up but breakage of the primary particles is not occurring.⁶ In a pressure titration, the PSD typically decreases with increasing dispersion pressure, due to the breakup of agglomerates and the attrition of primary particles at higher dispersion pressures. The proposal for the use of the VPAT (variable pressure attrition test) is that the rate of decrease of particle size with dispersion pressure, over the range 0.5–4 barg, will indicate how fragile the crystals are and therefore how likely they are to break during filtration. There is an assumption that over the range of dispersion pressures tested, we are seeing the attrition of primary particles, not the breakup of agglomerates, because relatively high dispersion pressures have been used.

Viriden⁷ presents two examples of pressure titrations where the particle size decreases with increasing dispersion pressure. By comparison with wet dispersion data it is possible to show that for one case breakup of agglomerates is achieved at 0.2 barg, and further decrease in the PSD is due to milling of the particles. The second case shows simultaneous milling and breakup of agglomerates. Milling of the primary particles is characterised by an increase in fines relative to that measured by wet dispersion. The dispersion pressures used in the pressure titration are also higher than those typically identified as suitable for sizing the drug substance (0.5–1 barg). Thus, testing the increase in fines at relatively high dispersion pressures is the best way to try and ensure that the decrease in particles size is due to attrition of particles and not breakup of agglomerates.

The VPAT procedure is then to size the particles using dispersion pressures of 0.5, 1, 2, 3, and 4 barg and the percentage of small material (f_s) recorded at each pressure, using the PSD at 0.5 barg as the reference to calculate x_{25} . The fractions of small particles f_s were calculated for all PSD and plotted against the square root of dispersion pressure for each compound. This resulted in straight lines, the gradient of which is referred to in this paper as the VPAT score.

The square root of dispersion pressure was chosen due to the following analysis. The probability of a collision occurring and resulting in breakage was estimated to be proportional to kinetic energy (v^2). The time spent in the sample chamber is inversely proportional to the velocity (v^{-1}). Hence, the overall probability of breakage is proportional to velocity. From Bernoulli’s equation, velocity is proportional to the square root of pressure.

RESULTS

Case Study 1: AZ1 at Lab Scale. The first compound evaluated is AZ1, an AstraZeneca development compound. The

structure is not relevant to the observations described in this paper. The data is from lab-scale investigations (~ 100 g scale, 2 L of crystallisation mass). Microscope pictures (Figure 2) show AZ1 to crystallise out in plates about $25\text{--}50\ \mu\text{m}$ wide and $>100\ \mu\text{m}$ long. The SEM image (Figure 3) allows the height to be

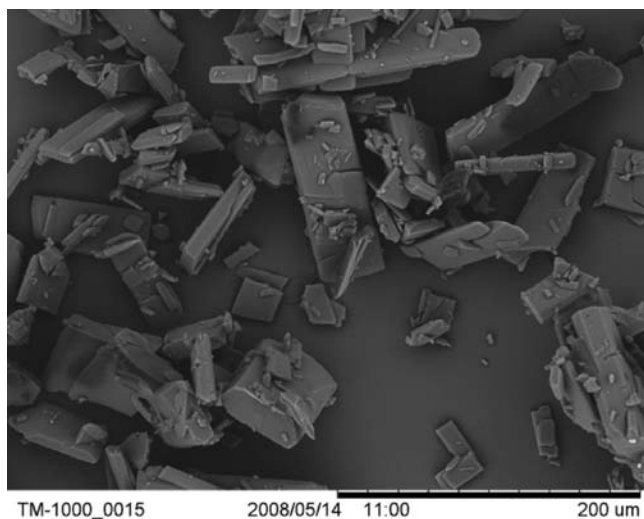


Figure 3. Scanning electron microscopy image of AZ1 after filtration (500 \times magnification).

estimated at $5\text{--}20\ \mu\text{m}$. The crystallisation mass was then filtered in the laboratory pressure filter by application of 2 barg pressure. The microscope pictures of a sample of the wet cake, after filtration, shows plates that have one jagged edge and appear to be the result of the fracture of a larger plate. The cake

was then dried by passing a stream of nitrogen through it overnight, then agitated for 2 h at 0.4 m/s tip speed. The microscope picture after drying looks qualitatively similar to that of the after filtration sample.

The microscope observations are confirmed by measured particles size distributions (Figure 4). Clearly there is a reduction in particle size after filtration at 2 barg. The subsequent drying and agitation activities seem to result only in small changes of the PSD, with slightly more fines appearing. Most of the change in PSD occurs during filtration.

Deagglomeration could also result in the decrease in particle size seen, as there is some agglomeration seen in the before filtration sample in Figures 2 and 3. From the data collected it is difficult to say conclusively if the reduction in particle size is solely due to fracture, or if some deagglomeration is also occurring. The Sympatec sizing method is designed to deagglomerate samples so the PSD should represent the size of mainly deagglomerated material. The presence of fractured edges in the optical microscope pictures points towards fracture rather than deagglomeration occurring. One method which could have been used to ascertain if deagglomeration was occurring would have been to size the particles using wet and dry dispersion and look for any differences in the PSD produced.

In Figure 5 we show the change of the fraction of small and large particles versus process coordinate. This graphical summary of the PSD demonstrates that the fraction of large particles (f_l) decreases from 23% to 14% after filtration and then stays almost constant when the particles are dried, but on agitating, it reduces further to 8%. Conversely, the fraction of small particles (f_s) increases from 23% to 38% after filtration,

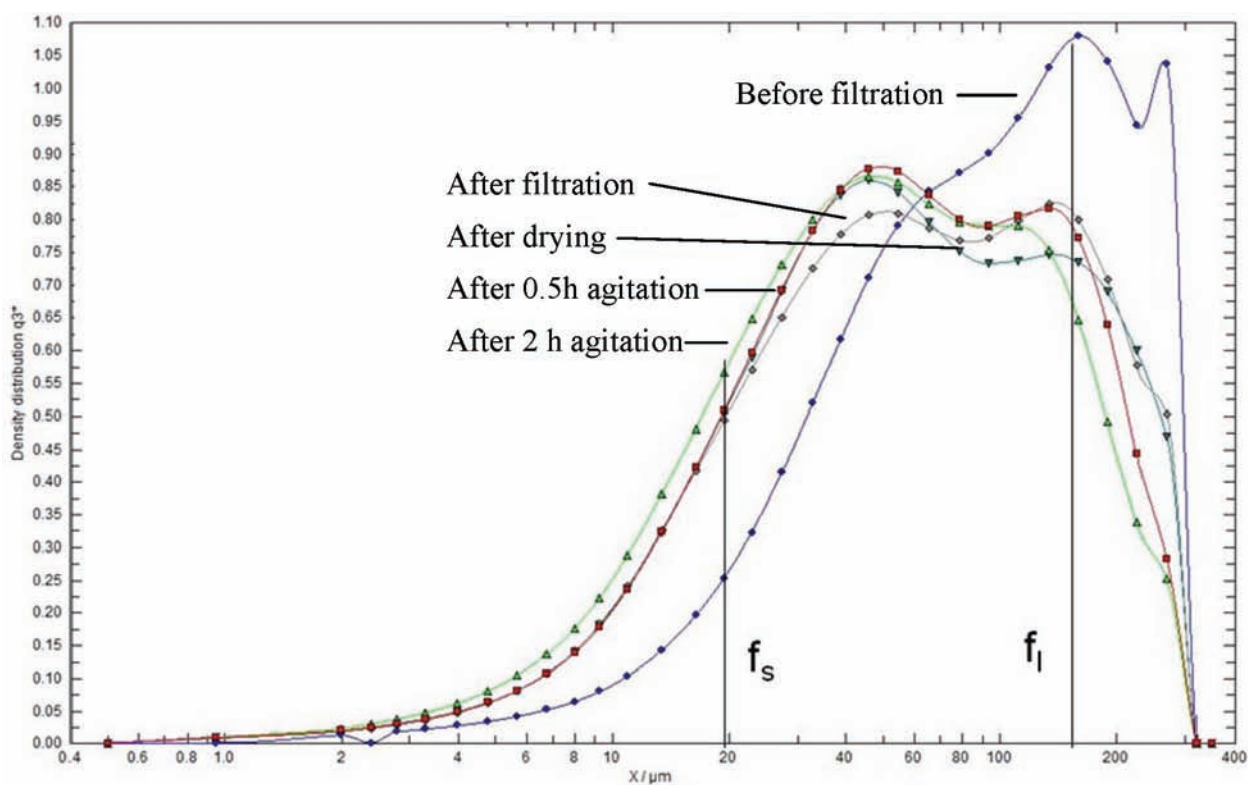


Figure 4. PSD of AZ1 before filtration, after filtration, after drying, and after 0.5 and 2 h agitation. Also drawn are lines that represent the boundary for the fraction of small particles (f_s : $<20\ \mu\text{m}$) and large particles (f_l : $>150\ \mu\text{m}$) as determined from the sample before filtration.

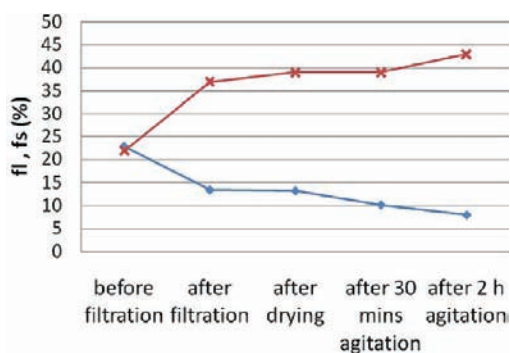


Figure 5. Changes in f_S and f_L of AZ1 on filtration and drying.

changes little during drying, and then increases by 4% to 42% after agitating.

Case Study 2: AZ2 at Pilot-Plant Scale. The initial laboratory-scale observations were confirmed at pilot-plant scale (20 kg, 400 L of crystallisation mass). AZ2 crystallises as plates with lengths 40–150 μm and width 5–10 μm as shown in Figure 6. The height was estimated as 5 μm . Microscope pictures of the samples before filtration, after filtration, and after agitated drying are shown in Figure 6. The PSD of all samples were measured. The fractions of small and large particles were calculated and plotted as functions of the process coordinate in Figure 7.

Figure 7 shows again a significant reduction in the fraction of large particles after the pressure filtration. No significant changes are seen during drying and agitation. The fraction of small particles (f_S) increases by 10% after filtration, with again no significant change during drying and agitating. A small decrease in fines can be observed between the after filtration and after agitation sample. This is assumed to be due to a sampling effect, as the after agitation sample was taken from bulk discharged product, and not directly from the filter. It is not possible to avoid this sampling effect (this compound is an intermediate; therefore, sampling procedures are not designed to account for segregation in the bed), which could influence the result. The overall effects seen on this compound isolated at pilot-plant scale are very similar to the effects seen for compound AZ1 isolated on the lab scale.

Further Evidence of Breakage during Pressure Filtration. After observing the impact of the pressure filtration on particle size of the crystals, a project was instigated to study this phenomenon in more detail. It was confirmed at lab scale on four commercially available compounds as well as two further AZ development compounds, one of these providing a

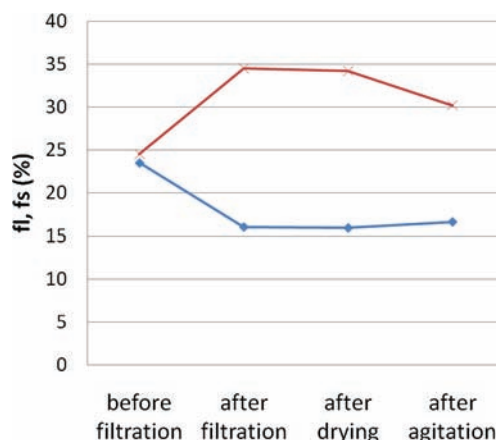


Figure 7. Changes in particle size as function of the isolation process coordinate.

further pilot-plant scale example. Table 2 shows a summary of further observations on the impact of pressure filtration, drying,

Table 2. Further observations of the impact of pressure filtration and drying on PSD of needle-shaped crystals

compound	scale (volume slurry/diameter pressure filter)	habit	decrease in % large crystals during fil- tration (%)	decrease in % large crystals dur- ing agitated drying (%)
aspirin	2 L/8 cm	rods	2	0
paracetamol	2 L/8 cm	plates	7	0
acetanilide	2 L/8 cm	plates	13	0
glutamic acid	2 L/8 cm	rods	6	0
glutamic acid	2 L/8 cm	needles	2	0
AZ1	2 L/8 cm	rods	11	6
AZ2	500 L/0.7 m	rods/ plates	8	2
AZ3	500 L/0.7 m	rods	7	0
AZ4	2 L/8 cm	tablets	0	18

and agitating on the PSD. All were conducted and analysed in the same manner as that of the two case studies described.

In summary, for nine systems evaluated we found that eight demonstrated a significant reduction in particle size on pressure filtration, with two having further particle size reduction observed during agitation and drying. This outcome was seen at both lab and pilot-plant scales. Only in one case, for a compound with blocky morphology (AZ4), did we observe no breakage during filtration, with attrition observed during

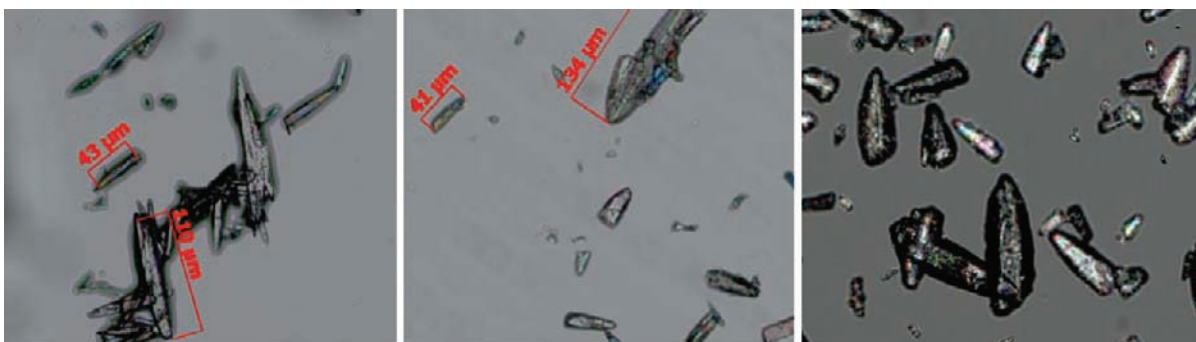


Figure 6. Microscope picture 10 \times magnification of AZ2 (left to right: before filtration, after filtration, and after agitation).

agitation. A SEM picture (300 \times magnification) of this compound is shown in Figure 8; optical microscope pictures

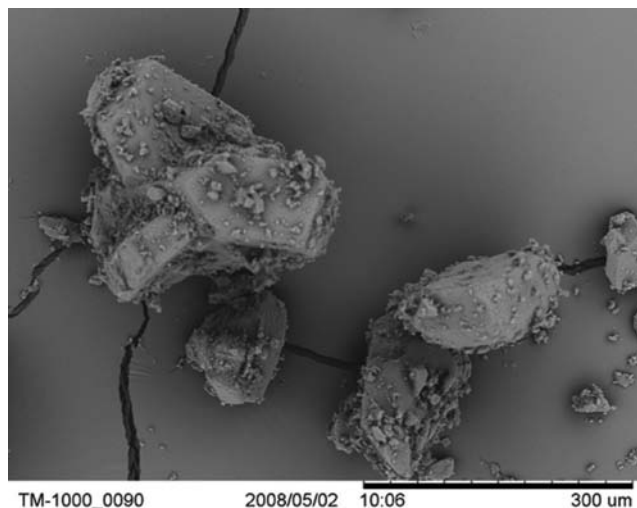


Figure 8. SEM (600 \times magnification) picture of crystals of AZ4 with blocky morphology.

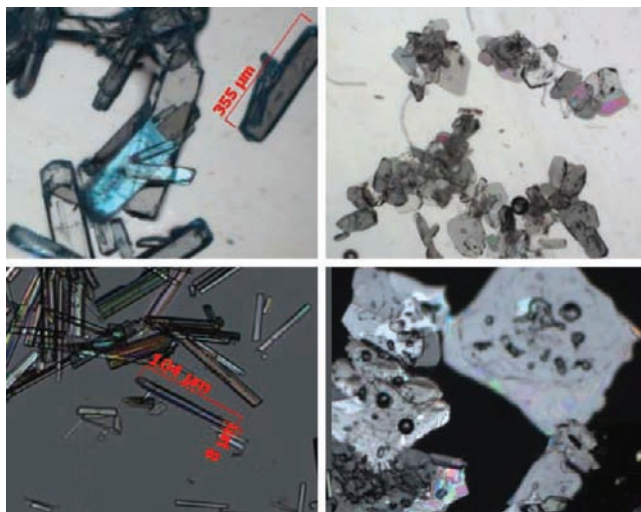


Figure 9. Microscope images (10 \times magnification) of aspirin, paracetamol, acetanilide, glutamic acid, and AZ3 (clockwise from top left). AZ1, AZ2, and AZ4 are shown elsewhere.

for the other compounds are shown in Figure 9. Therefore, it should be considered that breakage can occur both during pressure filtration as well as during agitated drying.

From Figure 9, aspirin and AZ3 are clearly not agglomerated in the initial sample, and still a decrease in particle size during filtration and drying is noted. Therefore, a fracture mechanism must be occurring, and decrease in particle size is not only due to deagglomeration.

There does not appear to be any reported examples of breakage during filtration reported in the literature. There are a few examples of breakage occurring during agitated drying. The study by Lekhal² on threonine found that after 180 min slurring at 0.2 m/s the average diameter reduced to 75% of the initial mean diameter. By comparison, the mean diameter of AZ1 is reduced to 64% of the initial diameter due to pressure

filtration. Subsequent agitation reduces this further to 60% of the initial mean diameter. The equipment in that study and the study presented here are of similar scale, but in the work by Lekhal² a pitched blade turbine was used as the agitator and vacuum as opposed to pressure filtration was used. No comparison of pre- and postfiltration PSD was presented, so it was not possible to compare the proportion of breakage occurring during filtration and agitated drying.

The two compounds evaluated at pilot-plant scale show trends of results very similar to those evaluated at lab scale. Therefore, the lab-scale representation of the pilot-plant scale pressure filter is likely to be representative. Significant differences between the pilot-plant and lab scale are that a higher torque is applied to the agitator on the pilot plant to move the larger volume of particles, the tip speed in the pilot plant is higher, and the particles are agitated before they are completely dry. The first two differences are unavoidable due to the limitations of the equipment involved. Agitating the particles while wet may result in less attrition being seen, as Lekhal² proposed that the lubricating effect of the solvent prevented attrition until the particles were completely dry. However, the filter cake is agitated for at least 15 min once dry before discharging to drums so attrition could occur during this phase of operation. The conditions in the lab-scale filter are sufficient to cause attrition of the particles during drying, if the particle material properties are suitable, as shown in the case of AZ4 where attrition during agitated drying is observed. In summary, the equipment used could cause attrition, but the main effect seen for these compounds tested is breakage during filtration.

A Fracture Model. There are two key mechanisms for breakage: (i) attrition, when small fragments are chipped off the ends of larger particles and (ii) fracture, where the particles are broken in two main fragments plus an amount of smaller fragments.⁸ Our observations are that the fraction of large particles reduces significantly. This suggests that fracture is the main breakage mechanism. Attrition would have resulted in the percentage of fines increasing more rapidly, with a smaller decrease in large particles.

A qualitative model has been produced to give an estimate of the magnitude of forces exerted on the particles due to the application of pressure. See Table 3 for a list of abbreviations used in the derivation of the model. This model is not intended as a mathematically rigorous model, and assumptions have been made to simplify the analysis. This model is also not rigorous in describing the direction of the breakage in the particle; it has been assumed that breakage occurs across the length of the particle. Finally, it has been assumed that all particles will settle such that the height is the smallest dimension—as drawn in Figure 11. A more thorough model is not practicable for us to develop or use within the time constraints of a drug development project.

In order to understand the forces that lead to the fracture of a crystal, it is assumed that the bed is in rest (no particle movement). The bed is modelled as a collection of solid beams that have on average three or more points of contact with other beams (as shown schematically in Figure 10). With only one or two points of contact, it is unlikely the bed is at rest.

In a pressure filter the initial slurry is subjected to a pressure of about 2 barg. The liquid flows through the bed and due to viscous drag, particles are subjected to a force.

As the particles remain at rest, the viscous forces are balanced by the force exerted by particle–particle contact. So for the

Table 3. Abbreviations used in the derivation of the model

symbol	definition	unit
A	cross sectional area	m^2
b	breadth of particle	m
C_c	concentration of contact points in a plane	$1/m^2$
C_j	concentration of junctions	$1/m^3$
C_p	concentration of particles	$1/m^3$
F_c	force on a contact point	N
h	height of particle	m
H	hardness	Pa
I	second moment of area	m^4
K_c	critical stress intensity factor	$Pam^{0.5}$
l_{br}	length of the broken fragment of particle	m
l_p	length of particle	m
M	bending moment	Nm
N	number of contact points per particle	–
P	pressure	N/m^2
v	velocity	m/s
V_p	volume of a particle (assumed cuboid = $L_p \times b \times h$)	m^3
z	distance from neutral axis	m
Δ	interparticle distance	M
ρ_b	bulk density	kg/m^3
ρ_t	true density	kg/m^3
σ_{crit}	critical stress required to break a particle	N/m^2
σ_{max}	maximum stress developed in a particle	N/m^2

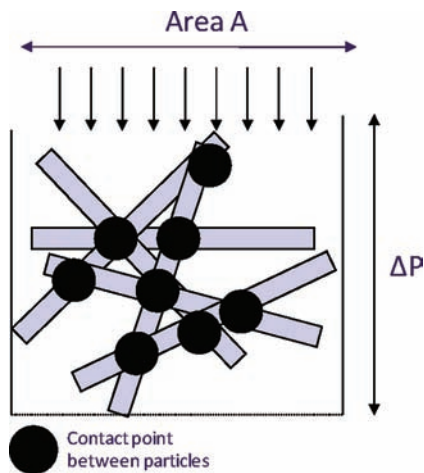


Figure 10. Schematic representation of the bed of particles.

cake to be able to resist pressure, the forces are transmitted through the filter cake via a network of contact points. These contact points will have a very small area compared to the total filter area; thus, the force on the particles generates a significant stress. If this stress exceeds the strength of the crystals, then the crystal can fracture. This fracture would typically occur along the slip plane. For the purposes of this analysis it is assumed that breakage will occur in the direction perpendicular to the longest dimension of the crystal.

The number of contact points may be estimated in a manner similar to that used by Muller.⁹ Muller calculated the yield strength of a network of crystals on the basis of the number per area of crystal-to-crystal junctions in a plane, and the strength of those junctions.

Similarly, in the case of the filter bed all the force exerted on the bed above a horizontal plane is transferred through only the contact points in that plane. If the concentration of contact points is C_c , then the number of contact points in a plane is

$C_c^{2/3}$. The concentration of contacts is simply approximated by particle concentration C_p , i.e. the number of particles per unit volume and the number of contacts per particle N_c :

$$C_c = C_p N_c \quad (1)$$

The concentration of particles in the bed is given by the bulk density of the dry bed divided by the average mass of a single particle:

$$C_p = \frac{\rho_b}{\rho_t V_p} = \frac{\rho_b}{\rho_t l_p b h} \quad (2)$$

The particle–particle distance, δ , is on average $C_p^{-1/3}$. The number of contacts per particle is therefore proportional to l_p/δ . The number of contacts per particle N_c is then:

$$N_c = l_p C_p^{1/3} \quad (3)$$

The force through each contact point follows from a force balance over the bed:

$$A \Delta P = A C_c^{2/3} F_c \text{ gives } F_c = \frac{\Delta P}{C_c^{2/3}} \quad (4)$$

If the particle is treated as a beam held in place by other particles (Figure 11) and assuming that the particle cannot move, then if the force on the particle exceeds its tensile strength, the crystal will break; one of the free ends would break due to the applied force.

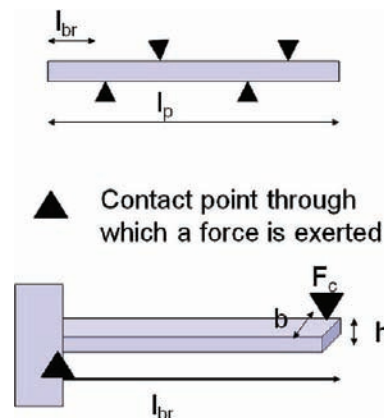


Figure 11. Representation of particle as a cantilever.

The length of the end that breaks, l_{br} , is dependent on the number of contacts per particle. Assuming that the contact points are equally spaced, the length of breakage is:

$$l_{br} = \frac{l_p}{N_c - 1} \quad (5)$$

which, if N_c is large, can be simplified to

$$l_{br} \approx \frac{l_p}{N_c} \quad (5a)$$

If it is now assumed that the length of crystal between two contact points behaves like a cantilever, supported at one end and a force applied at the other, then a stress will develop. This is shown in Figure 11.

The stress in the beam due to the bending moment is calculated from the Euler–Bernoulli beam theory as $\sigma = M_z/I$.

Table 4. Evaluation of the maximum stress in a range of habits used in this work

compound	habit	length (L_p μm)	height (h μm)	width (b μm)	change in f_1 after filtration (%)	σ_{max} (MPa)
aspirin	rods	400	5	60	2	11
paracetamol	plates	300	2	300	7	9
acetanilide	plates	300	2	300	13	9
glutamic acid	rods	500	5	10	6	17
glutamic acid	needles	300	5	10	2	13
AZ1	rods	400	5	40	11	11
AZ2	rods/plates	150	3	25	8	9
AZ3	rods	150	3	10	7	11
AZ4	tablets	400	100	100	0	3

The maximum stress, σ_{max} , occurs on the surface of the beam, at a distance $h/2$ from the neutral axis, and a distance l_{br} from the end of the crystal. If the stress in the beam σ_{max} exceeds a critical value σ_{crit} , then the crystal will break. The value of σ_{crit} will depend on the intrinsic mechanical properties of the material.

The maximum stress in the beam, where h the height, and the smallest dimension is vertical and l and b , the length and breadth, the longer dimensions are horizontal.

$$\sigma_{\text{max}} = \frac{6l_{\text{br}}F_c}{bh^2} \quad (6)$$

This approach is similar to that of Grof¹⁰ where the breakage of needle shaped particles under compression was modelled. Discrete element models were set up to model particle–particle forces between randomly orientated particles under compression. Particles would break if the bending in the particle reached a threshold value.

Combining eqs 1, 2, 4, 5a, and 6 gives the maximum stress in the particle related to the dimensions of the particle, the applied pressure, and the ratio between bulk and the true density of the particle:

$$\sigma_{\text{max}} \approx 6 \frac{\Delta P l_p^{5/9}}{\left(\frac{\rho_b}{\rho_t}\right)^{11/9} b^{-2/9} h^{7/9}} \quad (7)$$

This can be further approximated to:

$$\sigma_{\text{max}} \approx 6\Delta P \left(\frac{\rho_t}{\rho_b}\right) \left(\frac{l_p}{h}\right)^{0.5} \left(\frac{h}{b}\right)^{0.2} \quad (8)$$

Equation 8 suggests the σ_{max} increases, and thus the particle is more likely to break when the bulk density decreases, the pressure drop increases, the length of the particle increases, and particle height decreases.

On the basis of eq 8, the maximum stress developed in the particles studied were calculated using particle dimensions from microscopy and bed densities as measured (Table 4). Taking the particle dimensions from microscopy is not ideal, but for the purposes of estimating the stress in a particle of a typical size, the reliability is satisfactory. The values range from 3–17 MPa, which is close to the range of tensile strength of some typical pharmaceutical materials (5–14 MPa¹¹). The maximum stress in the material increases with length of the needle. The stress developed in a more tabletlike crystal is reduced.

The maximum stress in the particle does not correlate with the amount of breakage seen, defined by the change in f_1 after filtration. This is because the particles have different intrinsic

strengths. Therefore, dimensions of the particle alone are not sufficient to predict how much breakage will be observed during filtration.

Prediction of Particle Breakage. In order to make a prediction with respect to particle fracture, not only the dimensions of the particle are required, but also the tensile strength. Although this can be measured,¹¹ equipment for doing so is not readily available. Rather than measuring σ_{crit} we used data from the pressure titration.

As an example, the PSDs obtained by sizing AZ1 at different dispersion pressures are shown in Figure 12a. There is a significant change in the PSDs with increasing dispersion pressure. The plot of f_s against square root of dispersion pressure is shown in Figure 12b.

Plotting the VPAT score against the extent of breakage observed during pressure filtration gives a weak positive correlation (Figure 13).

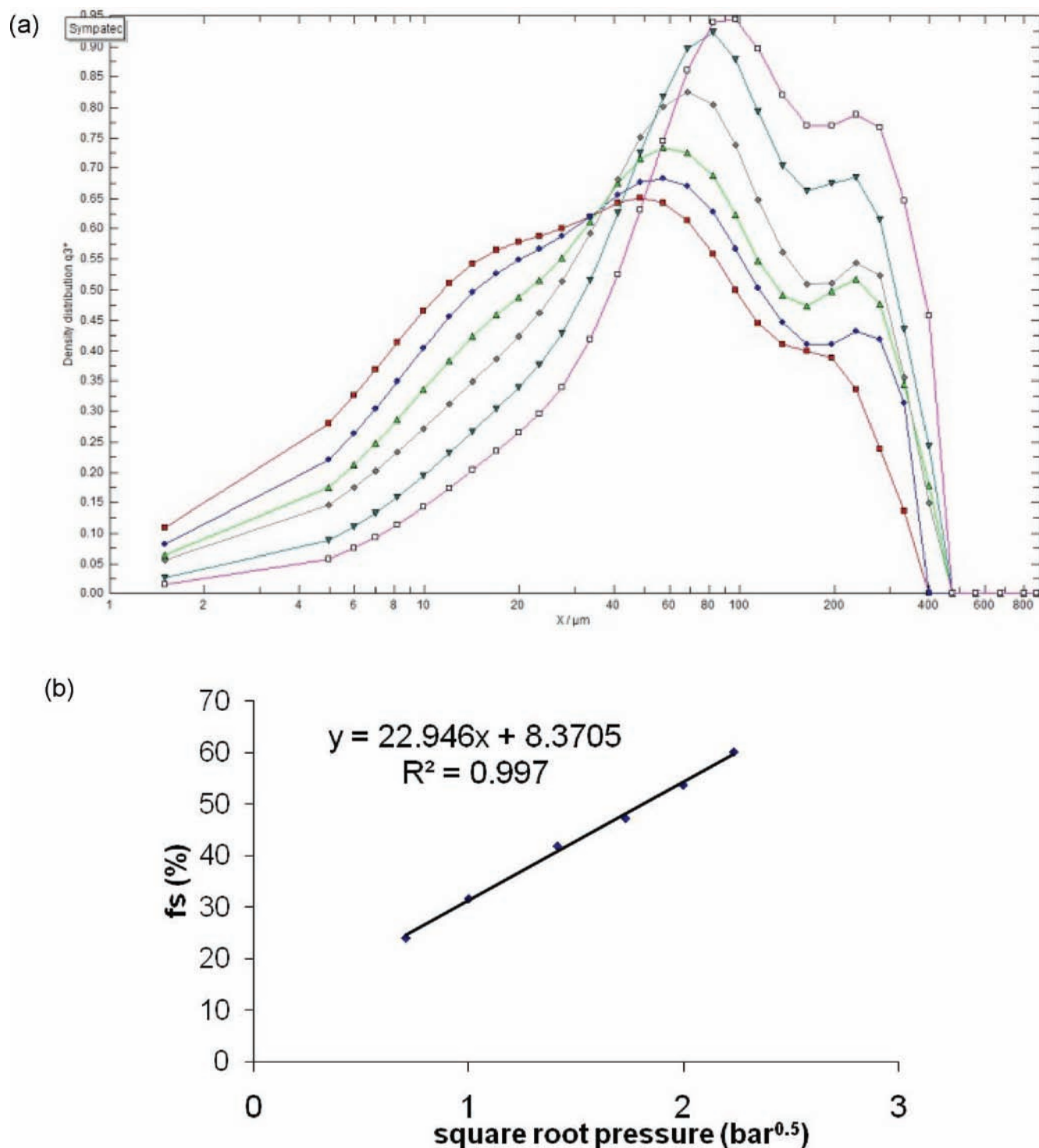
The mode of breakage is different in dry dispersion; the particle will hit the walls and other particles, and the breakage seen will be more likely to be attrition. Attrition observed due to impact results from material properties different from those of breakage due to applied pressure. The propensity for attrition to occur for semi-brittle materials is shown in the equation below.¹²

$$\eta = \frac{\rho v^2 l H}{K_c^2}$$

Therefore knowledge of at least three different material properties (H , K_c , and σ_{crit}) plus the dimensions of the particles would be required to investigate the relationship between results from the VPAT test and breakage during filtration and drying. For the purposes of using it is a tool to identify potentially fragile compounds, where more work in understanding the effect of filtration and drying on particle size is required, this test is suitable and has been used on additional development compounds. This method had so far only been tested on a limited number of compounds, the majority having a high aspect ratio, and we would not anticipate that this result is general across the full range of particle dimensions and material properties.

CONCLUSIONS

It is common knowledge that the PSD of a crystallisation mass can change significantly after isolation and drying and that the change in PSD on scale up is not well predicted. It was commonly thought that agitation while drying was the main cause of crystal fracture. The data gathered in this paper clearly demonstrate the novel finding that for the needle-shaped systems tested, fracture occurs during filtration, and some



further breakage during agitation and drying is also observed. Therefore, the impact of both filtration and drying on PSD should be considered when developing an isolation process for a new development compound.

The main changes in PSD for these compounds are observed during pressure filtration, and this holds at both laboratory and pilot-plant scale. Deagglomeration could also be at least partially responsible for the reduction in particle size seen, but further work, including comparison of sizing by wet and dry

dispersion methods would be required to completely elucidate this.

Mechanistic understanding has been developed to understand why particles would break under applied static pressure. The stresses to which the particles are subjected on being filtered at 2 barg are shown to be of the same order of magnitude as the measured tensile stress of pharmaceutical materials.

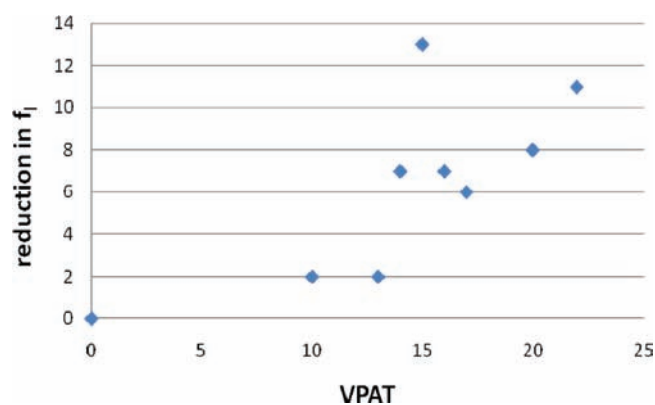


Figure 13. Correlation between VPAT score and breakage observed during filtration.

A small-scale test has been developed, using the decrease in particle size with dispersion pressure as an indication of the fragility of the compounds. This test is useful to prompt further development work on a compound which will potentially break during filtration and drying. More work is required to understand why those needle-shaped compounds were found to break mainly during filtration, while it has been demonstrated that other compounds break by attrition during agitated drying.

AUTHOR INFORMATION

Corresponding Author

Claire.macleod@astrazeneca.com.

Notes

The authors declare no competing financial interest.

ACKNOWLEDGMENTS

We thank Andrew Wiersum and Ross McCluckie for their assistance with the experimental work.

REFERENCES

- (1) Kim, S.; Lotz, B.; Lindrud, M.; Girard, K.; Moore, T.; Nagarjan, K.; Alvarez, M.; Lee, T.; Nikfar, F.; Davidovich, M.; Srivastava, S.; Kiang, S. Control of the particle properties of a drug substance by crystallization engineering and the effect on drug product formulation. *Org. Process Res. Dev.* **2005**, *9*, 894–901.
- (2) Lekhal, A.; Girard, K.; Brown, M.; Kiang, S.; Khinast, J.; Glasser, B. The effect of agitated drying on the morphology of l-threonine (needle-like) crystals. *Int. J. Pharm.* **2004**, *270*, 263–277.
- (3) Muller, F. L.; Fielding, M.; Black, S. N. A Practical Approach for Using Solubility to Design Cooling Crystallisations. *Org. Process Res. Dev.* **2009**, *13*, 1315–1321.
- (4) Sandler, N.; Wilson, D. Prediction of granule packing and flow behavior based on particle size and shape analysis. *J. Pharm. Sci.* **2010**, *99*, 958–968.
- (5) Lekhal, A.; Girard, K.; Brown, M.; Kiang, S.; Glasser, B.; Khinast, J. Impact of agitated drying on crystal morphology: KCl-water system. *Powder Technol.* **2003**, *132*, 119–130.
- (6) International Organization for Standardization *Particle Size Analysis: Laser Diffraction Methods*; ISO: Geneva, Switzerland, 2009; p 13320.
- (7) Virden, A. Method Development for Laser Diffraction Particle Size Analysis. *Pharm. Technol.* **2010**, 100–106.
- (8) Bemrose, C. R.; Bridgewater, J. A Review of Attrition and Attrition Test Methods. *Powder Technol.* **1987**, *49*, 97–126.
- (9) Muller, F. L. On the Rheological Behaviour of Batch Crystallisations. *Chem. Eng. Res. Des.* **2009**, *87*, 627–632.

(10) Grof, Z.; Kohout, M.; Stepanek, F. Multiscale Simulation of Needle Shaped Particles Breakage under Uniaxial Compression. *Chem. Eng. Sci.* **2007**, *62*, 1418–1429.

(11) Roberts, R.; Rowe, R.; York, P. The Relationship between the Fracture Properties, Tensile Strength and Critical Stress Intensity Factor of Organic Solids and Their Molecular Structure. *Int. J. Pharm.* **1995**, *125*, 157–162.

(12) Ghadiri, M.; Zhang, Z. Impact Attrition of Particulate Solids. Part 1: A Theoretical Model of Chipping. *Chem. Eng. Sci.* **2002**, *57*, 3659–3669.